

Received March 23, 2020, accepted April 5, 2020, date of publication April 17, 2020, date of current version May 4, 2020.

Digital Object Identifier 10.1109/ACCESS.2020.2988611

PSO-GWO Optimized Fractional Order PID Based Hybrid Shunt Active Power Filter for Power Quality Improvements

ALOK KUMAR MISHRA¹, SOUMYA RANJAN DAS², (Graduate Student Member), PRAKASH K. RAY³, (Senior Member, IEEE), RANJAN KUMAR MALLICK¹, ASIT MOHANTY³, (Member, IEEE), AND DILLIP K. MISHRA⁴, (Graduate Student Member)

¹Department of Electrical and Electronics Engineering, SOA Deemed to be University, Bhubaneswar 751030, India

²Department of Electrical Engineering, International Institute of Information Technology (IIIT), Bhubaneswar 751003, India

³Department of Electrical Engineering, College of Engineering and Technology (CET), Bhubaneswar 751003, India

⁴School of Electrical and Data Engineering, University of Technology Sydney, Sydney, NSW 2007, Australia

Corresponding author: Prakash K. Ray (pkray@cet.edu.in)


ABSTRACT This paper presents a Hybrid Shunt Active Power Filter (HSAPF) optimized by hybrid Particle Swarm Optimization-Grey Wolf Optimization (PSO-GWO) and Fractional Order Proportional-Integral-Derivative Controller (FOPIDC) for reactive power and harmonic compensation under balance and unbalance loading conditions. Here, the parameters of FOPID controller are tuned by PSO-GWO technique to mitigate the harmonics. Comparing Passive with Active Filters, the former is tested to be bulky and design is complex and the later is not cost effective for high rating. Hence, a hybrid structure of shunt active and passive filter is designed using MATLAB/Simulink and in real time experimental set up. The compensation process for shunt active filter is different from predictable methods such as $(p-q)$ or (i_d-i_q) theory, in which only the source current is to be sensed. The performance of the proposed controller is tested under different operating conditions such as steady and transient states and indices like Total Harmonic Distortion (THD), Input Power Factor (IPF), Real Power (P) and Reactive Power (Q) are estimated and compared with that of other controllers. The parameters of FOPIDC and Conventional PID Controller (CPIDC) are optimized by the techniques such as PSO, GWO and hybrid PSO-GWO. The comparative simulation/experiment results reflect the better performance of PSO-GWO optimized FOPIDC based HSAPF with respect to PSO/GWO optimized FOPIDC/CPIDC based HSAPF under different operating conditions.

INDEX TERMS Fractional order proportional-integral-derivative controller (FOPIDC), harmonic compensation, hybrid shunt active power filter (HSAPF), particle swarm optimization-grey wolf optimization (PSO-GWO), power quality.

I. INTRODUCTION

Nowadays in almost all applications, power electronics based loads such as uninterruptible power supply (UPS), switched mode power supply (SMPS), adjustable speed drives (ASD) etc. are being used. All of these power electronics based equipments draw the current from the supply which is of non-linear in nature and produce a lot of harmonics [1]. Due to this non-linear current, the utility system has to supply a quite large amount of reactive power from the supply. Since, the current drawn from the supply is not at all sinu-

soidal, and the source voltage and current are not in phase, the systems and loads connected at the Point of Common Coupling (PCC) are affected due to the harmonics [2], [3]. In order to overcome the bad effects of harmonics, various solutions exist; out of which one is passive filter [4]. Regardless of many advantages, passive filters are not so much effective in some conditions like transients, presence of higher order harmonics, resonance issues and have large size, and fixed compensation characteristics [5]–[7]. A new power electronics interfacing device is developed by the researchers called Active Power Filters (APFs) for reactive power and harmonic compensations and to overcome the demerits of passive filters [4], [8].

The associate editor coordinating the review of this manuscript and approving it for publication was Eklas Hossain .

The basic concept of active power filters (APFs) is that they inject the compensating current with equal magnitude and opposite sign, into the power system in order to cancel out the harmonics [9]–[11]. Comparing with various APF topologies, SAPF [12], [13] is the most popular one as compensation of current harmonics is vital in all most all industrial applications [14], [15]. For a SAPF controller, the researchers have developed many control strategies [16]–[23]. The controller used in SAPF has two most important parts, one of them is extracting the reference current [24]–[28] and the other is PWM pulse generation for inverter [29]. In this paper, a HSAPF is designed by a low rated shunt active power filter (SAPF) and a low cost shunt passive filter. To extract the reference current for the SAPF, many control techniques such as instantaneous power theory ($p-q$) or synchronous reference frame theory (i_d-i_q) are available in the literature [30]. Present paper focused on a novel control method to estimate the current references which do not require the load reactive volt-ampere [31]. To control the inverter dc voltage of the capacitor and to extract the maximum value of current references, CPIDC or FOPIDC is applied [32]. CPIDC is the most extensively utilized controller in industries as it can easily applicable and its design is simple [33]. It doesn't generally give a powerful control to non-linear, dubious, and coupled systems. With a lot of advantages, it sometimes fails to give its robustness and disturbance elimination properties [34]. Traditionally, the integer order controllers dominate the entire field of control theory. Due to the research interest in fractional calculus, FOPID is tested to be more effective in different applications as compared to CPIDC. Compared to the CPIDC, the five parameters (K_p , K_d , K_i , α , β) where α and β are fractions for providing an improved tuning and performance. The aim of the tuning technique is to locate the ideal parameters of the CPIDC and FOPIDC as per requirements. In the literature, various tuning methods are available for optimizing the parameters of CPIDC and FOPIDC [35]–[39].

Nowadays evolutionary and swarm methods are used for controller parameter optimization which are encouraged by animal's nature and evolution concept like PSO algorithm [40] to optimize the parameters of SAPF [41]. Grey Wolf Optimization (GWO), which are inclined by hunting process of Grey Wolves recently published in [42], and is used to optimize the UPFC controller parameters [43]. PSO is a basic and powerful method and can be executed effectively. Yet, when dealing with a heavy constraint optimization, it may get trapped in local minima. Whereas, GWO can balance between exploitation and exploration very effectively, it can also avoid trapping in local optima. So, hybrid PSO-GWO algorithm is proposed in this work for optimal setting of the parameters used in CPIDC and FOPIDC [44]. Similarly, different current control methods are proposed for SAPF to generate the switching pulse [45], [46], but for better controllability and fast response, Hysteresis Current Control (HCC) PWM method are very popular [47]. Hence, in this work, HCC PWM method is used.

The highlights of the current work are to:

- Develop a Simulink model of a HSAPF.
- Design FOPIDC for estimation of the maximum value of current reference.
- Optimize the control parameters of CPIDC/ FOPIDC using PSO/GWO and PSO-GWO techniques.
- Estimate the control actions of the FOPIDC under steady state, transient, balanced and unbalanced loading conditions.
- Compare the performances to certify the better response of the optimized FOPIDC based HSAPF.
- With the obtained optimized controller parameters, a laboratory prototype of HSAPF system is developed with analog based FOPIDC to verify the simulation results.

This paper is structured in the following manner. Section II discusses the structure and modeling of HSAPF system. The control algorithms and optimization techniques are given in Section III. Section IV gives the detailed simulation results and analysis under balanced and unbalanced loading conditions. Prototype hardware results are presented in Section V. Conclusions and future scopes are given in Section VI.

II. MODELLING OF HYBRID SHUNT ACTIVE POWER FILTER

The HSAPF is formulated by the help of passive and active filters. The hybrid structure improves the compensation characteristics of the filter that minimizes the demerits of active and passive filters while providing the advantages of both. Hence, a robust HSAPF is proposed in this paper by incorporating voltage source PWM converter and LC passive filter. The HSAPF connected to power system is shown in the Figure 1.

The laboratory prototype is designed and tested under various conditions. The parameters of the shunt LC filter are optimized to reduce the harmonics present because of the non-linear loads. It is observed that the existing 5th, 7th and 11th order harmonics are reduced to great extent. Here, compensating filtering characteristics of passive and active filters are coordinated to provide better performance under different operating situations. In this work, a unity power factor along with reduction in current harmonics is taken as the compensation objective. A combination of storage system, DC link capacitor and switches with anti-parallel diodes are structured so as to filter out the harmonics contents. Based on the requirements, a compensating current by the voltage source converter (VSC) is injected at point of common coupling (PCC) to eliminate the harmonics. If only active filters are used, then the power rating required for PWM converter is more, hence, a passive filter is used in addition to active filter to compensate the dominant harmonics. In order to reduce the cost, PWM converter is designed using power MOSFETs in place of IGBTs.

At PCC, equal magnitude with opposite polarity harmonic current has to be injected in order to accomplish harmonic compensation. This in turn improves the power quality in

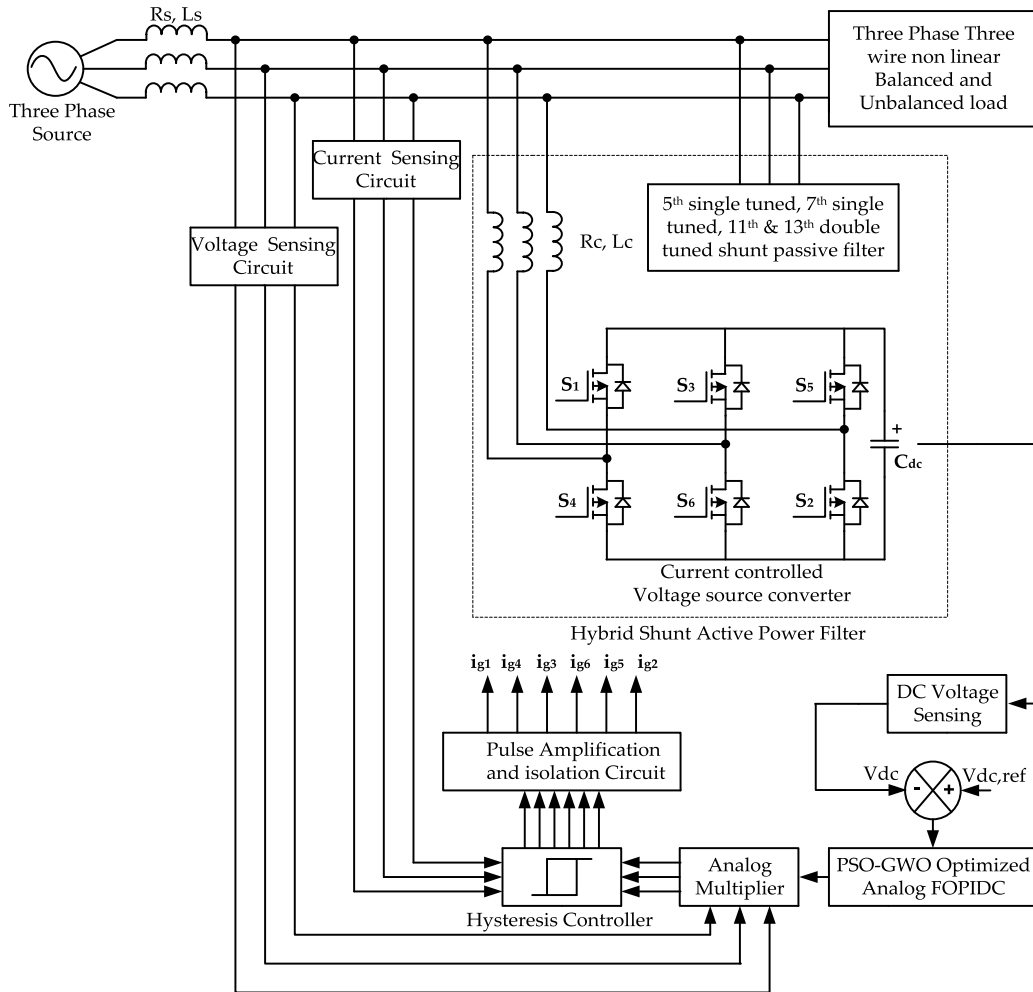


FIGURE 1. Schematic diagram of hybrid shunt active power filter.

the distribution systems by cancelling the original distortions. Basic configuration of shunt active power filter (SAPF) connected with the power system at PCC is shown in Figure 2. As shown, the inductance L_c helps to suppress the harmonics in the system. The instantaneous source current can be represented as:

$$i_s(t) = i_L(t) - i_{af}(t) \tag{1}$$

The source voltage is represented as:

$$V_s(t) = V_m \sin \omega t \tag{2}$$

In case if the load is nonlinear, load current is having harmonic component as well as fundamental component that can be represented as:

$$i_L(t) = \sum_{n=1}^{\infty} I_n \sin(n\omega t + \varphi_n) = I_1 \sin(\omega t + \varphi_1) + \left(\sum_{n=2}^{\infty} I_n \sin(n\omega t + \varphi_n) \right) \tag{3}$$

The instantaneous load power can be calculated as:

$$p_L(t) = v_s(t) * i_L(t) = V_m I_1 \sin^2 \omega t * \cos \varphi_1 + V_m I_1 \sin \omega t * \cos \omega t * \sin \varphi_1 + V_m \sin \omega t * \left(\sum_{n=2}^{\infty} I_n \sin(n\omega t + \varphi_n) \right) \tag{4}$$

$$p_L(t) = p_f(t) + p_r(t) + p_h(t) . \tag{5}$$

This load power is having harmonic, reactive and active power. From Eq. (4), the real power drawn from the load is represented as:

$$p_f(t) = V_m I_1 \sin^2 \omega t * \cos \varphi_1 = v_s(t) * i_s(t) \tag{6}$$

If the active filter gives the harmonic and reactive power, then the source current $i_s(t)$ will be purely sinusoidal and in phase with the source voltage. The three-phase source currents after compensation can be expressed as:

$$i_{sa}^*(t) = \frac{p_f(t)}{v_s(t)} = I_1 \cos \varphi_1 \sin \omega t = I_{\max} \sin \omega t . \tag{7}$$

where $I_{\max} = I_1 \cos \varphi_1 =$ peak value of reference current.

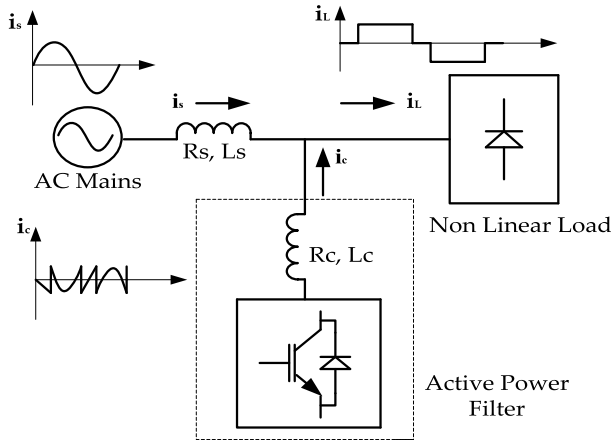


FIGURE 2. Basic configuration of shunt active power filter.

Similarly,

$$i_{sb}^*(t) = I_{max} \sin(\omega t - 120^\circ) \quad (8)$$

$$i_{sc}^*(t) = I_{max} \sin(\omega t + 120^\circ) \quad (9)$$

PSO/GWO/PSO-GWO optimized FOPIDC/CPIDC is used to estimate I_{max} and regulate the dc link capacitor voltage.

III. OVERVIEW OF CONTROLLERS AND OPTIMIZATION TECHNIQUES

A. CPIDC

The Proportional, Integral, and Derivative actions are applied to $e(t)$ (error signal) in a PID controller, again which is applied to the plant model. Mathematically, PID controller is represented in Eq. (10).

$$u(t) = K_p e(t) + K_i \int_0^t e(t) + K_d \frac{de(t)}{dt} \quad (10)$$

The above control parameters (K_p, K_i, K_d) are optimized using PSO, GWO and hybrid PSO-GWO techniques.

B. FOPIDC

The basic block diagram of HSAPF with FOPID controller is as shown in Figure 1. Here, the error signal $e(t)$ helps to produce the control signal $u(t)$. The Transfer Function (TF) of the proposed FOPID controller is [32]:

$$TF = K_p + \frac{K_i}{s^\alpha} + K_d s^\beta \quad (11)$$

where, α and β represent the fractional orders of the integrator and differentiator and K_p, K_i and K_d denote the proportional, integral, and derivative gains of the proposed of FOPID controller respectively.

The steps required for designing the controller are:

1. Regulate K_p for reducing the rise time and steady-state error.
2. Regulate K_d for reducing the overshoot and settling time.
3. Regulate K_i for eliminating the steady-state error.

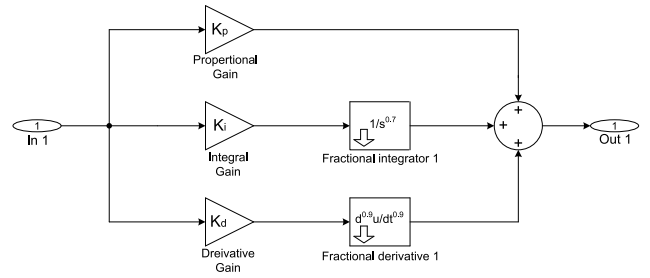


FIGURE 3. Simulink diagram of FOPIDC.

TABLE 1. The optimal values of control parameters (for PSO-GWO).

K_p	K_d	K_i	α	β
18	6	1.5	0.7	0.9

4. Regulate K_p, K_i, K_d, α , and β to get the desired output.
5. The configuration of FOPIDC is presented in Figure 3.
6. The optimal parameters of FOPIDC are obtained using PSO, GWO and hybrid PSO-GWO techniques and are presented in Table 1 (for PSO-GWO).

C. PARTICLE SWARM OPTIMIZATION (PSO) TECHNIQUE

One of the simplest and popular optimization is PSO. In this technique, a number of particles are allowed to move in a multidimensional search space [40]. Each particle velocity is to be updated while searching:

$$v_i^{k+1} = \omega v_i^k + c_1 rand_1 (P_{i,pbest}^k - x_i^k) + c_2 rand_2 (P_{i,gbest}^k - x_i^k) \quad (12)$$

where ω is the initial weight which varies between 0.4 to 0.9, two random variables are selected $rand_1$ and $rand_2$ that are varying in the range of [0,1] and the acceleration coefficients are c_1 and c_2 . The swarm position is updated by

$$x_i^{new} = x_i + v_i \quad (13)$$

With more iteration, the most excellent solution can be obtained that is given by

$$x_i^{k+1} = \left\{ \begin{array}{l} x_{i,new} iff (x_{i,new} \leq f(x_i)) \\ x_{i,otherwise} \end{array} \right\} \quad (14)$$

D. GREY WOLFS OPTIMIZATION (GWO) TECHNIQUE

This GWO is a recent metaheuristic technique based on the swarm cleverness which is motivated by the mind set of Grey-Wolf while they are hunting a prey [42]. Grey wolves stay in a pack and are placed in a position to execute the hunting procedure. To model the hunting process mathematically, the best fittest solution is given to the α group of wolves which are followed by β, γ and δ groups. The wolves make a loop around the victim to initiate the hunting of the prey, which is given as:

$$\vec{D} = \left| \vec{C} \cdot \vec{X}_P(t) - \vec{X}(t) \right| \quad (15)$$

$$\vec{X}(t+1) = \left| \vec{X}_P(t) - \vec{A} \cdot \vec{D} \right| \quad (16)$$

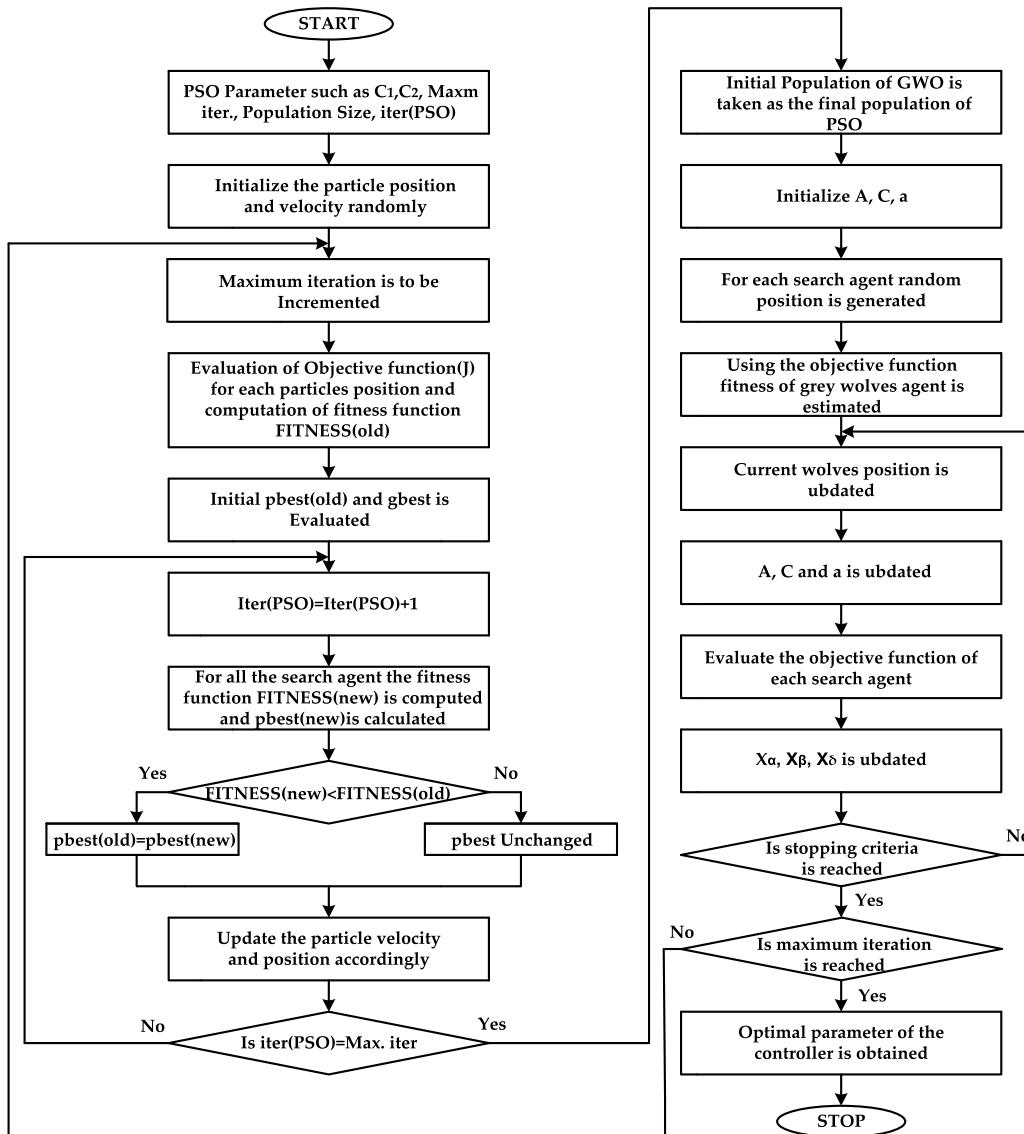


FIGURE 4. Flow chart for PSO-GWO algorithm for finding the optimal controller parameters.

In equation (16) ‘*t*’ represents the current iteration. *X* and *X_p* vectors represent the Grey wolf and the victim position respectively where *A* and *C* are the coefficient vectors given in equations (17) and (18).

$$\vec{A} = 2 \cdot \vec{a} \cdot \vec{r}_1 - \vec{a} \tag{17}$$

$$\vec{C} = 2 \cdot \vec{r}_2 \tag{18}$$

In equations (17)-(18), *r*₁ and *r*₂ represent the random vector which varies in the range of [0, 1] and the component ‘*a*’ decreases from 2 to 0 during the iteration. The hunting process can be formulated as

$$\vec{D}_\alpha = \left| \vec{C}_1 \cdot \vec{X}_\alpha - \vec{X} \right|, \vec{D}_\beta = \left| \vec{C}_2 \cdot \vec{X}_\beta - \vec{X} \right|, \vec{D}_\delta = \left| \vec{C}_3 \cdot \vec{X}_\delta - \vec{X} \right| \tag{19}$$

$$\vec{X}_1 = \vec{X}_\alpha - \vec{A}_1 \cdot \left(\vec{D}_\alpha \right), \vec{X}_2 = \vec{X}_\beta - \vec{A}_2 \cdot \left(\vec{D}_\beta \right), \vec{X}_3 = \vec{X}_\delta - \vec{A}_3 \cdot \left(\vec{D}_\delta \right) \tag{20}$$

The average value of positions of *α*, *β* and *δ* wolves are found to be the most excellent position of prey which is given as

$$\vec{X}(t+1) = \frac{\vec{X}_1 + \vec{X}_2 + \vec{X}_3}{3} \tag{21}$$

E. HYBRID PSO-GWO TECHNIQUE

The PSO technique has the demerit of being trapped to the local minima when it is subjected to a heavy constraint, though it has some advantages such as its simplicity, robustness and it can be implemented easily. On the other

TABLE 2. THD, real, reactive power and power factor in various cases.

Different Condition	Different Parameter					
	THD %			P (kW)	Q (VAR)	Cos ϕ
	Phase-a	Phase-b	Phase-c			
Without any filter	25.47	25.48	25.47	8.631	511.1	0.9671
Passive filter connected alone	15.27	14.34	17.20	8.679	-1637	0.9712
PSO-CPIDC HSAPF System	3.75	2.82	4.24	9.156	19.16	0.9921
GWO-CPIDC HSAPF System	3.57	3.17	3.19	9.173	34.39	0.9979
PSO-GWO-CPIDC HSAPF System	3.52	3.42	3.33	9.157	23.35	0.9921
PSO-FOPIDC HSAPF System	2.58	2.48	2.48	8.731	18.29	0.9919
GWO - FOPIDC HSAPF System	1.89	1.95	1.96	8.718	8.583	0.9966
PSO-GWO - FOPIDC HSAPF System	1.64	1.69	1.71	8.718	0.3022	0.9982

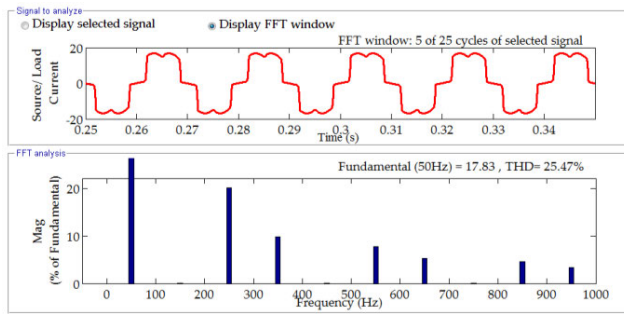


FIGURE 5. Load current waveform and its harmonic spectrum without any filter.

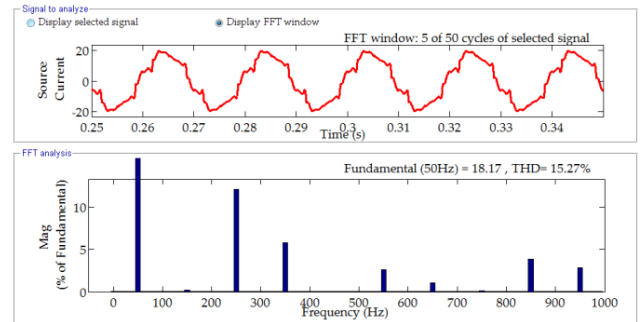


FIGURE 6. Source current waveform and its harmonic spectrum when passive filter connected alone.

hand, GWO avoids being trapped locally and it keeps a balance between exploration and exploitation. In this way, both these extraordinary highlights of PSO and GWO are combined in the algorithm of hybrid PSO-GWO. Figure 4 represents the flow chart of Hybrid PSO-GWO algorithm and

the following steps explain the execution of PSO-GWO method.

1) PSO OPERATION

Step1: The fitness function of all the particles are evaluated.

Step2: Individual P_{best} and global G_{best} are computed.

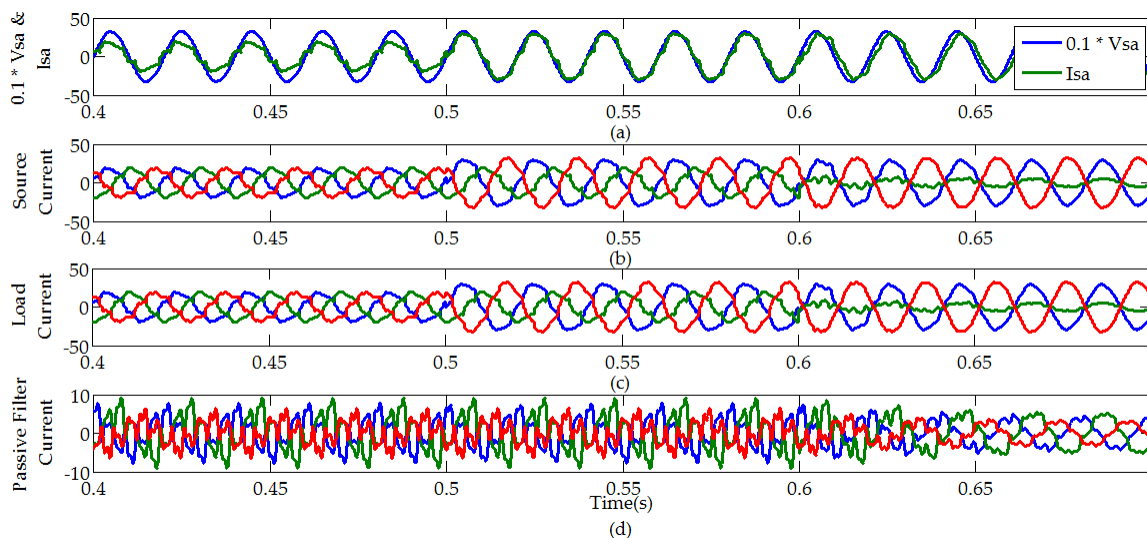


FIGURE 7. Various waveforms with passive filter system.

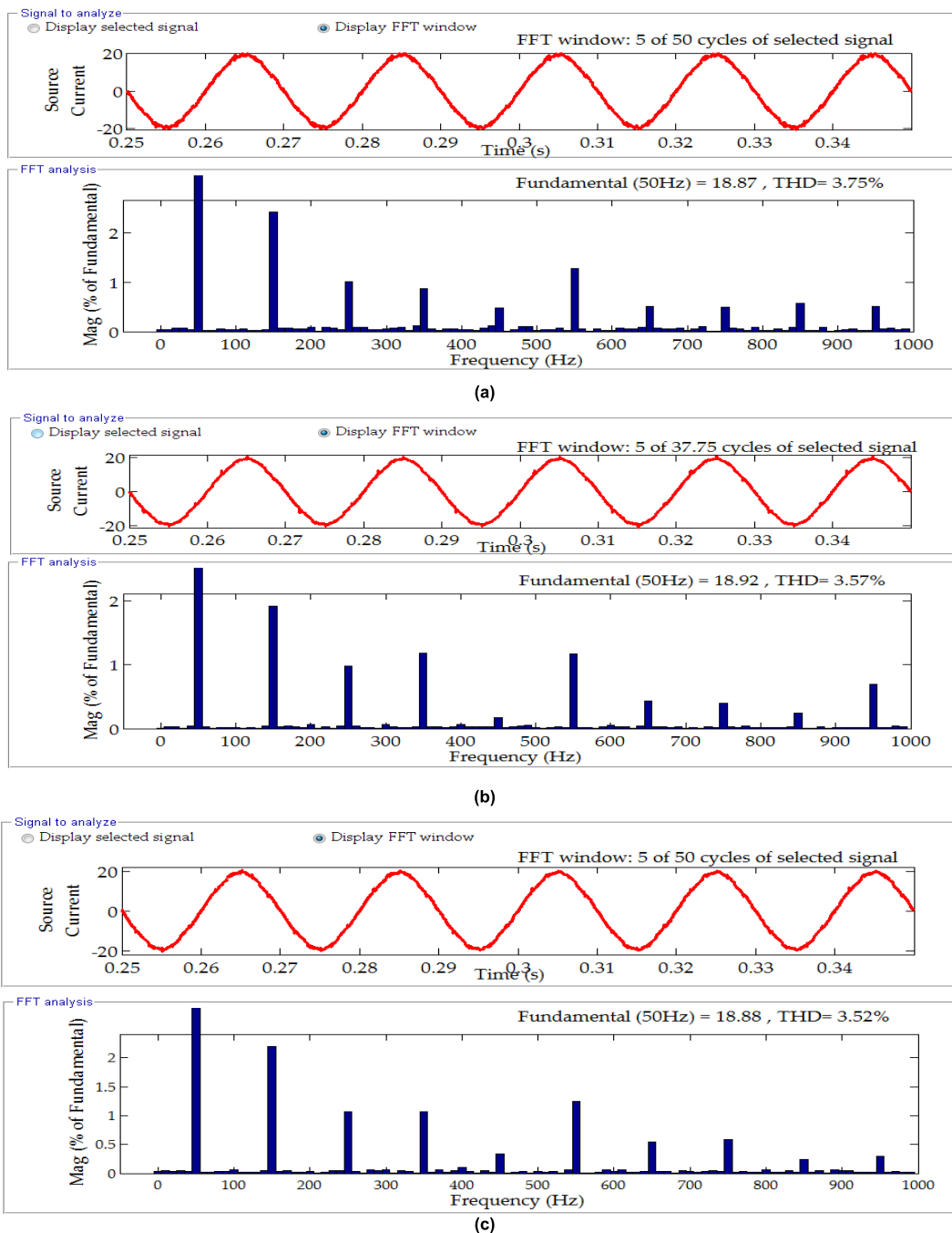


FIGURE 8. Source current waveform and its harmonic spectrum for a) PSO optimized, b) GWO optimized c) PSO-GWO optimized CPIDC based HSAPF.

Step3: Using equation (12), each swarm velocity is updated.

Step4: Using equation (13), swarm position is being updated.

Step4: Fitness values of each particle is computed.

Step5: Using equation (14), the best solution is selected for the next iteration with the comparison of fitness value of each particle.

2) GWO OPERATION

Step6: The initial population of GWO is the final population of PSO.

Step7: Using equations (17), (18) the parameter A , C and a are updated.

Step8: Random position is generated for each search agent.

Step9: For the Grey wolves, the fitness values are calculated using the objective function.

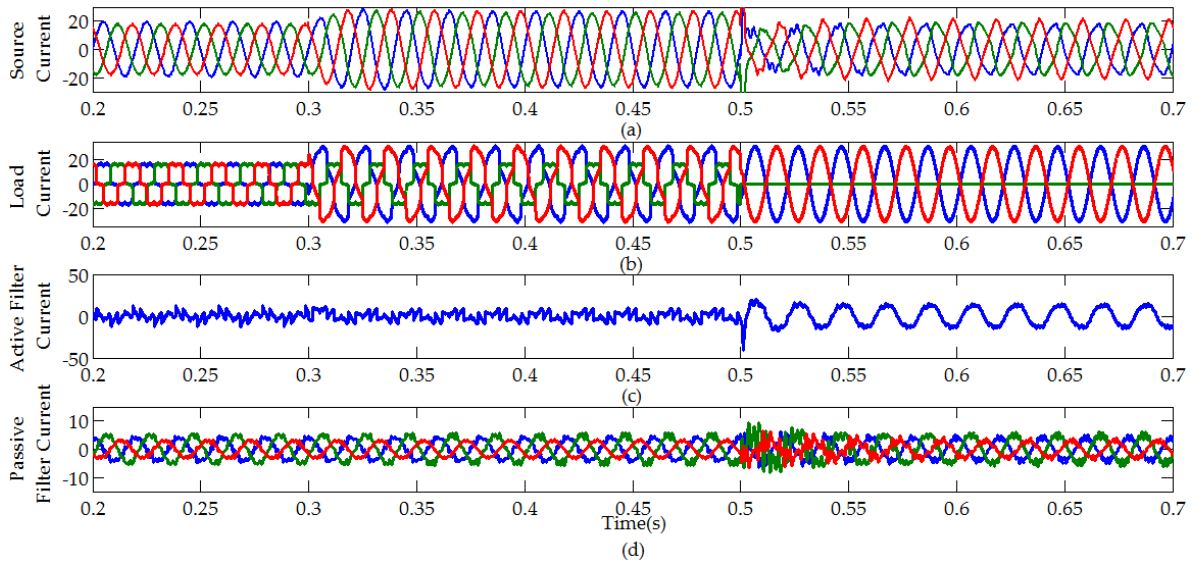


FIGURE 9. Various waveforms for PSO-GWO optimized CPIDC based HSAPF system.

Step10: The position of Grey wolves are updated and also the parameters A , C and a are updated.

Step11: By comparing the fitness functions, best solution is chosen for next iteration.

Step12: The best solution is to be chosen for further iteration by comparing with the fitness functions.

Step13: X_α , X_β and X_δ are updated.

Step14: The above steps are repeated till the stopping criterion is reached.

Step15: Final optimal controller parameters are obtained.

F. OPTIMIZATION PROBLEM FOR DC LINK VOLTAGE REGULATION

At steady state, the VSI of the SAPF should not deliver any reactive power or it should not take up any reactive power. The fundamental concern lies here is to get an optimized CPIDC or FOPIDC which makes the dynamics of the dc link voltage (V_{dc}) very low. Ziegler-Nichols tuning method is popularly used for tuning of CPIDC and needs wide-ranging experimentation. Hence, there is always possibility of better tuning of CPIDC or FOPIDC to improve the settling time and overshoot. This intention can be consummated by using PSO-GWO optimization technique which reduces the deviation of V_{dc} from the reference value V_{dc}^* . The rise time (t_r), Maximum Overshoot ($\Delta V_{c\max}$) and the steady state error (E_{ss}) are the imperatives that infer the optimality of a CPIDC or FOPIDC. To decrease the dc link voltage deviation (ΔV_{dc}) is the main objective here which is given as

$$\Delta V_{dc} = V_{dc}^* - V_{dc} \quad (22)$$

A non constrained type optimization problem with the objective function (J) given in equation (23) is chosen in this paper with performance criteria of integral square error (ISE). In equation (23), t_0 , t_s represent the starting and settling

time respectively where α , β are the weighing factors. The importance of α weighing factor is to reduce E_{ss} the steady state error whereas β decides the value of $\Delta V_{c\max}$ and t_s . Smaller β value indicates that the settling time is reduced and large β value results in less overshoot.

$$J = \int_0^t (\Delta V_{dc})^2 dt = \beta \Delta V_{dc\max} + (1 - \beta) (t_s - t_0) + \alpha \cdot |E_{ss}| \quad (23)$$

IV. SIMULATION RESULTS AND ANALYSIS

For the simulation analysis of Hybrid Shunt Active Power Filter (HSAPF), a Simulink model is developed to investigate the performance under balance and unbalance loading conditions. Here, a three phase diode bridge rectifier with resistive load on its DC side is taken as the non-linear load for which filtering is required. For unbalance loading, a resistive load is connected between phase-a and phase-c, and for complete unbalance case phase b is open. First shunt passive filters are designed based on the characteristic of the load current. Then, a shunt active power filter is connected for better compensation. The inverter with a DC link capacitor and energy storage system helps during the transients. Resistance is connected in series with the inductance for better compensation. For designing the passive filters, the reactive power requirement is taken as 2kVAR which is taken as 1000 VAR for single tuned 5th harmonic filter and 500 VAR each for single tuned 7th harmonic filter and double tuned filter. The various parameters of the hybrid filter are given in Table 3 in Appendix. The load current waveform and its harmonic spectrum are as shown in the Figure 5. The load current is having a THD of 25.48% with dominant 5th, 7th, 11th and 13th harmonics. For this load, analysis is performed

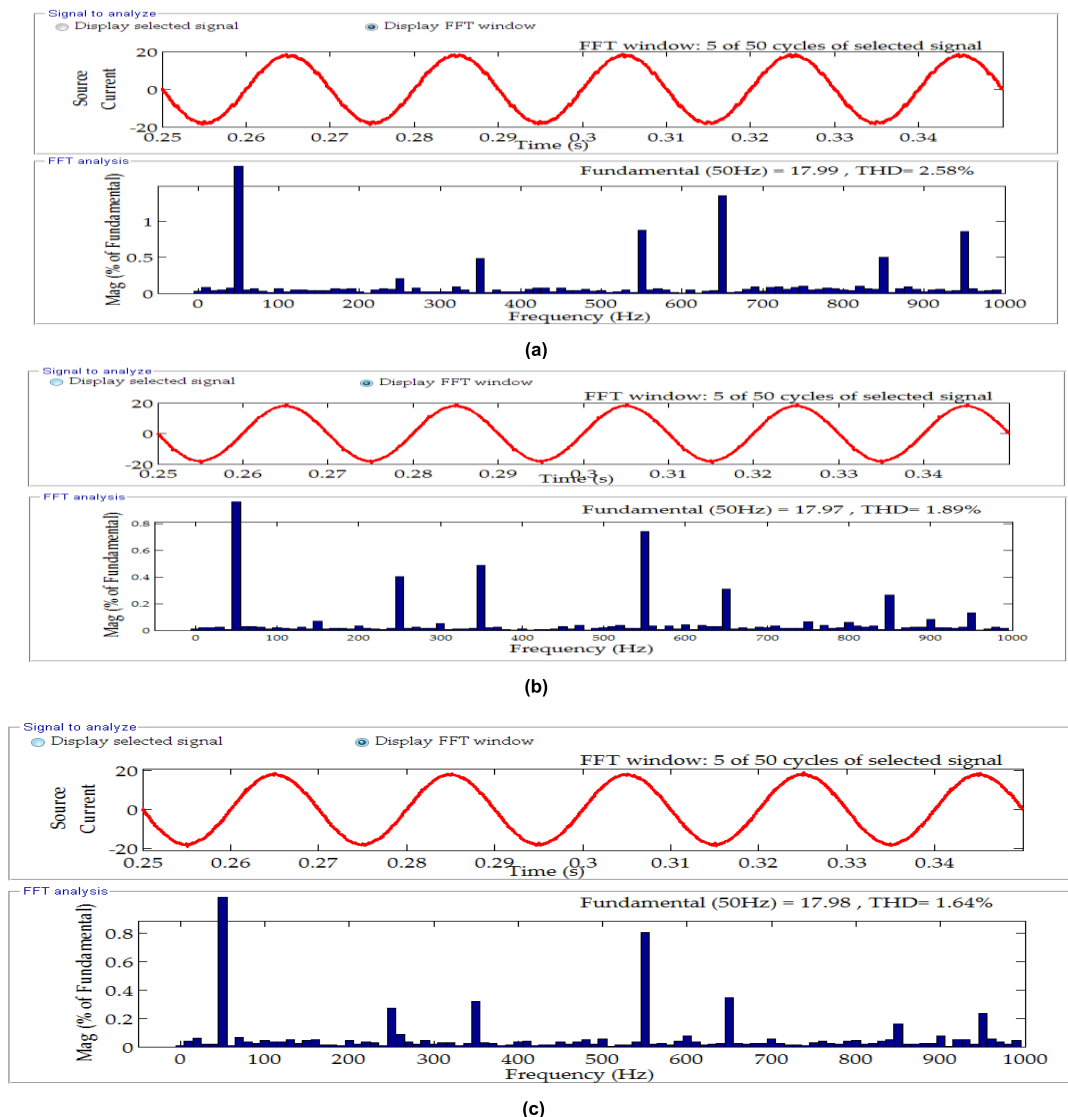


FIGURE 10. Source current waveform and its harmonic spectrum for a) PSO optimized, b) GWO optimized c) PSO-GWO optimized FOPIDC based HSAPF system.

in three cases. Case 1: when passive filters are connected alone. Case 2: when HSAPF is connected to the system with optimized CPIDC for estimating the maximum value of reference current. Case 3: when HSAPF is connected to the system with Optimized FOPIDC used for estimating the maximum value of reference current.

A. WHEN PASSIVE FILTER ARE CONNECTED ALONE

Now, for this load, the designed passive filters are shunted and the source current wave shape is as shown in the Figure 6. From Figure 6, it can be seen that the THD is reduced from 25.47% to 15.27%. The source voltage, current, load current and passive filter current waveforms, obtained under balance and unbalance loading conditions, are shown in the Figure 7. It is analyzed that the source voltage and current are improved by the action of the passive filter.

B. OPTIMIZED CONVENTIONAL PID CONTROLLED HSAPF SYSTEM

The THD of the source current and the performance can be improved by appending the SAPF into the existing passive filter system. From Figure 6 and Figure 7, it is clear that the performance parameter (THD) is not satisfactory, hence PSO/GWO/PSO-GWO Optimized CPIDC based SAPF is connected to the system. Source current along with its harmonic spectrum is given in Figure 8 (a)-(c). Among different optimized CPIDC, PSO-GWO optimized one gives better result, with THD of 3.52 %, as compared to PSO or GWO Optimized CPIDC, with THDs of 3.75 % and 3.57 % respectively. The waveforms of source current, load current, active and passive filter currents for this case are depicted in Figure 9 (a)-(d) respectively.

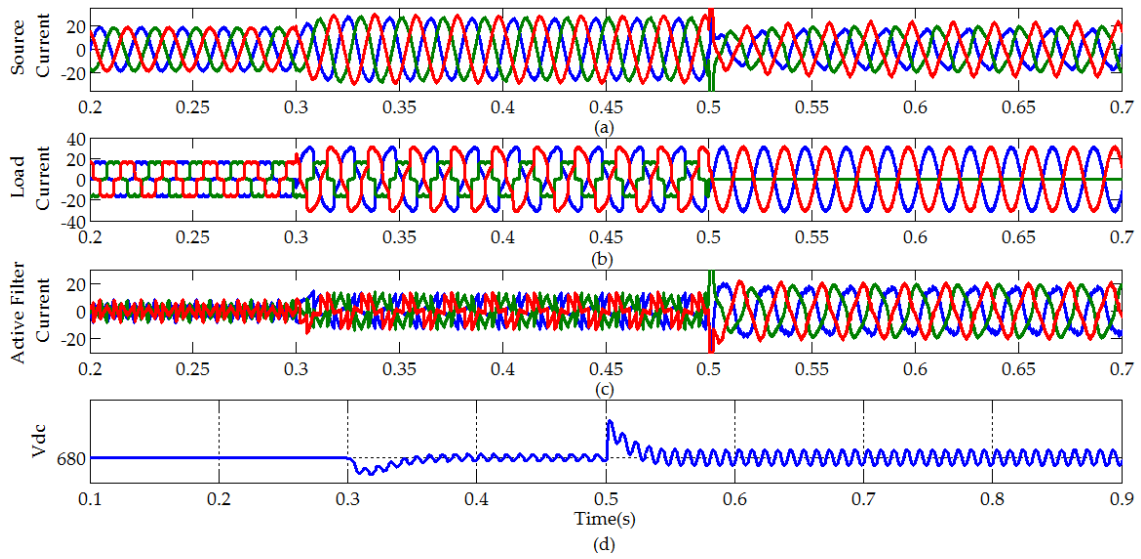
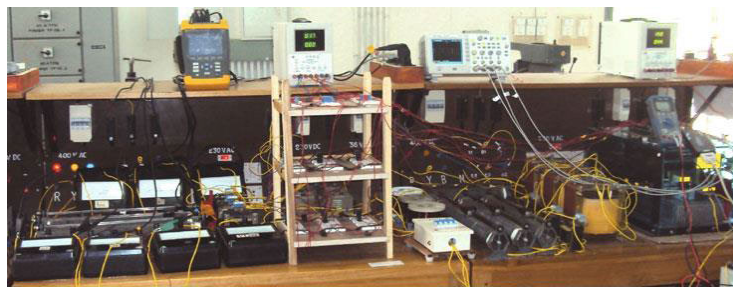
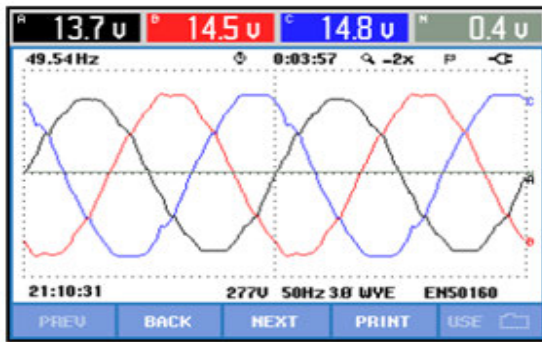


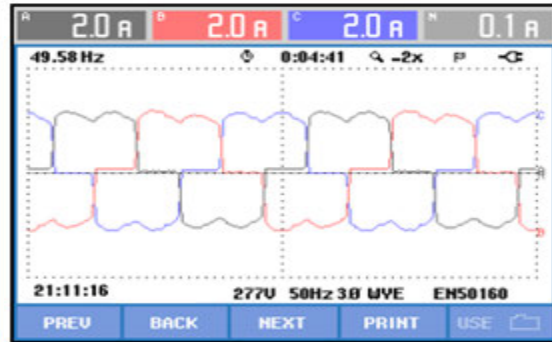
FIGURE 11. Various waveforms of PSO-GWO optimized FOPIDC based HSAP system.



(a)



(b)



(c)

FIGURE 12. (a) Experimental set up (b) source voltage and (c) source current without any filter.

C. OPTIMIZED FRACTIONAL ORDER PID CONTROLLED HSAPF SYSTEM

The different waveforms with THD using PSO, GWO and PSO-GWO optimized FOPIDC based HSAPF is shown in Figure 10 (a)-(c). From Figure 10, we can see that the THD of the source current is reduced from 25.47% to 1.64% by installing PSO-GWO optimized FOPIDC based HSAPF as compared to 2.58 % and 1.89 % respectively for PSO and GWO optimized FOPIDC based HSAPF. The source current, load current, filter current and dc link voltage waveforms,

under both balance and unbalance condition, are obtained as shown in Figure 11 (a)-(d).

For unbalance condition at t=0.3 secs, a load resistance of 40Ω is connected between phase-a and phase-c, and at t=0.5 secs, phase-b is opened to check the single phasing condition. From Figure 11(a)-(b), we can see that after t=0.3 secs, load current is unbalanced, but the load draws a nearly balance current from the source due to the presence of HSAPF. From Figure 11(d), we can analyze that the capacitor voltage is regulated at 680V which is the reference value

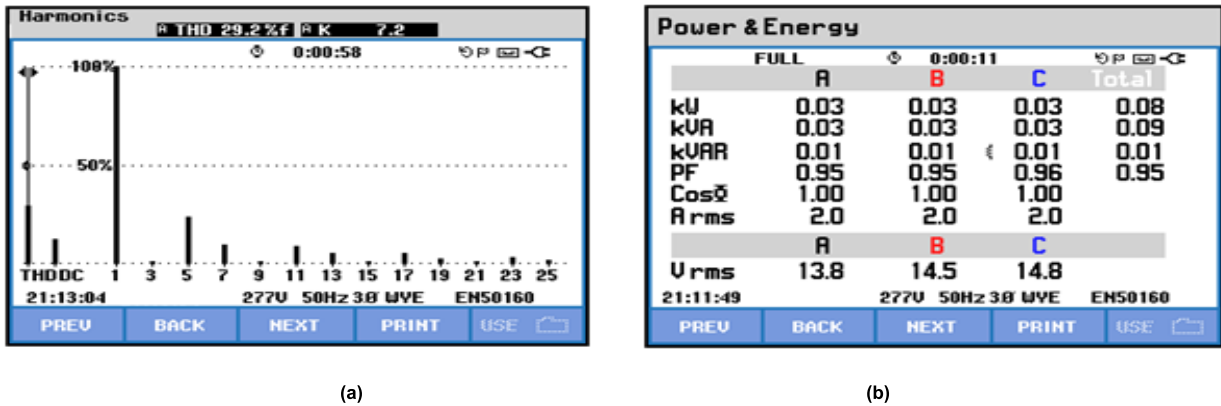


FIGURE 13. (a) Harmonic analysis of phase-a source current (b) Performance parameters without any filter.

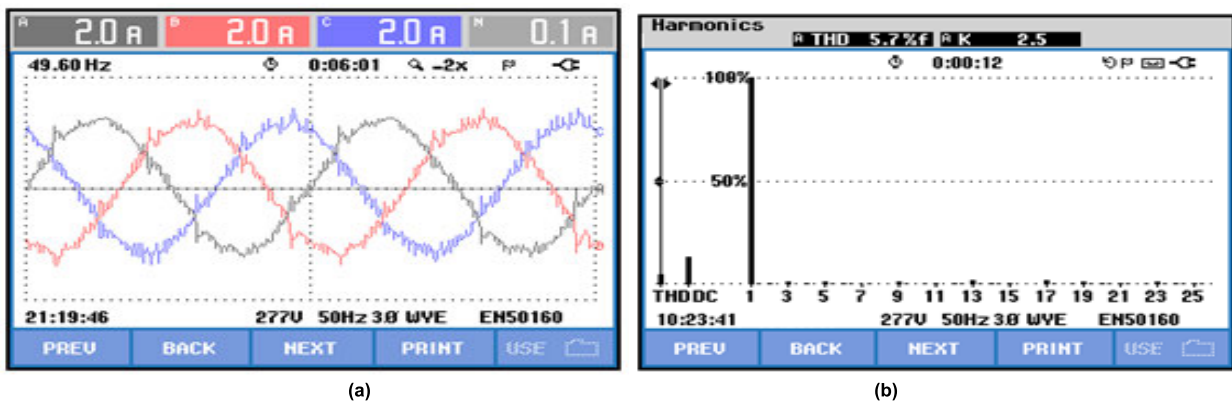


FIGURE 14. (a) Three phase source current (b) Harmonic spectrum of phase-a source current for PSO-GWO Optimized FOPIDC based HSAPF.

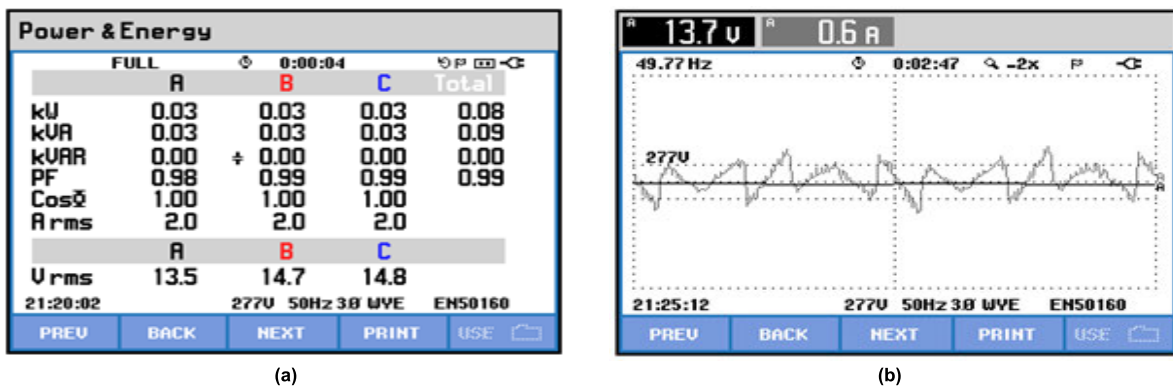


FIGURE 15. (a) Performance parameters HSAPF (b) Injected filter current using PSO-GWO Optimized FOPIDC based HSAPF.

under balance and unbalance loading conditions. We can also observe that the THD of the PSO-GWO optimized FOPIDC based HSAPF is 1.64% when compared to PSO-GWO optimized CPIDC based HSAPF of 3.52% and that of passive filter case with THD of 15.27%. The source current THD, Real power (P), Reactive power (Q) and Power factor Cos ϕ are calculated for different cases and are given in Table 2. These results indicate that the reactive power is compensated

and power factor is improved by HSAPF and hence improves the power quality in the distribution system.

V. EXPERIMENTAL RESULTS AND ANALYSIS

With the obtained optimal value FOPIDC, an analog controller based prototype of the HSAPF system is developed, as shown in Figure 12 (a), by integrating the power circuit and the control hardware, and tested in the laboratory

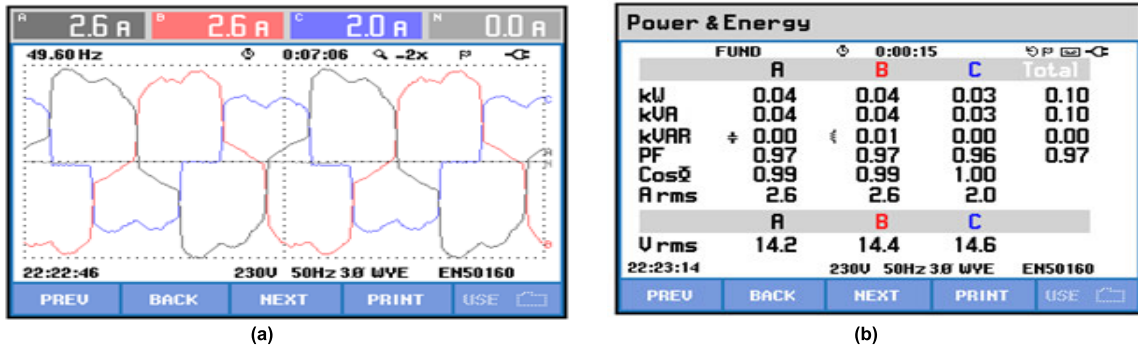


FIGURE 16. (a) Unbalanced load current. (b) Performance parameter under unbalanced loading condition using the proposed hybrid filter.

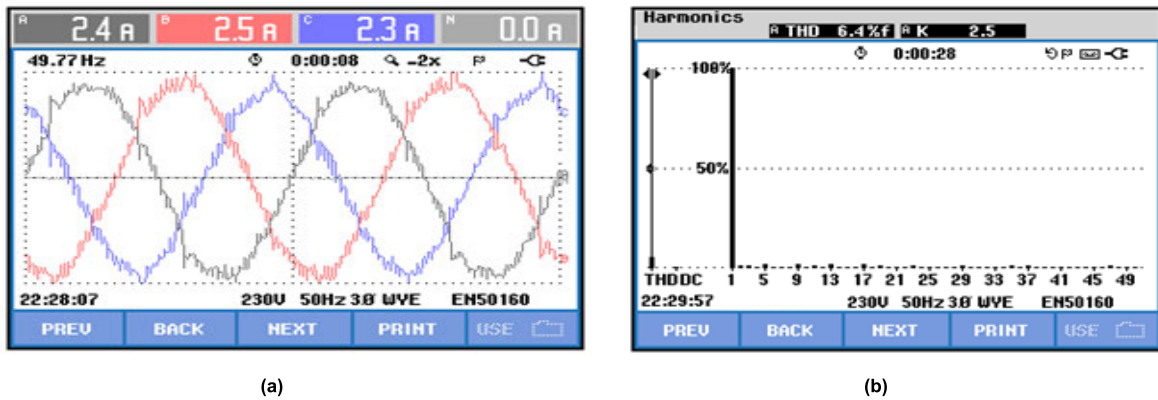


FIGURE 17. (a) Balanced source current after compensation (b) harmonic spectrum of phase-a source current using the proposed hybrid filter.

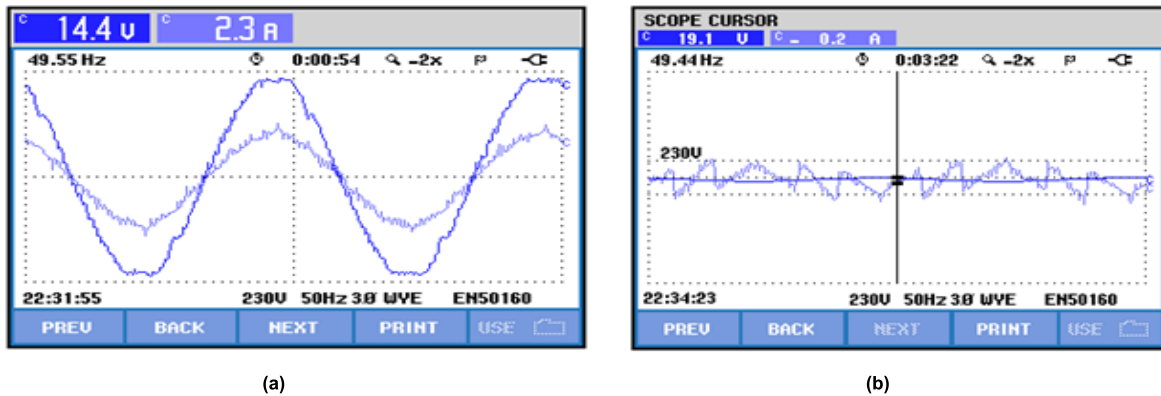


FIGURE 18. (a) In phase source current and voltage after compensation using the proposed hybrid filter (b) Injected filter current.

to verify the simulation results. The performance of the system is investigated experimentally for various loading conditions. Parameters selected for the experimental verification are given in Table 4. All experimental results are recorded with the help of a fluke power quality analyzer. For these experiments, the load used is a diode bridge with lamp load on its DC side. Figure 12 (b)-(c) shows the three phase source voltage, source current without any filter.

From Figure 12, it is clear that the current drawn by the diode rectifier is non-sinusoidal. The frequency spectrum is as shown in the Figure 13 (a), which consists of significant 5th, 7th, 11th and 13th harmonics. Figure 13 (a)-(b) shows the THD of phase-a source current and the performance parameters. THD of the three phases are found to be 29.2%, 28.4%, 27.8% respectively for phase-a, phase-b, phase-c respectively.

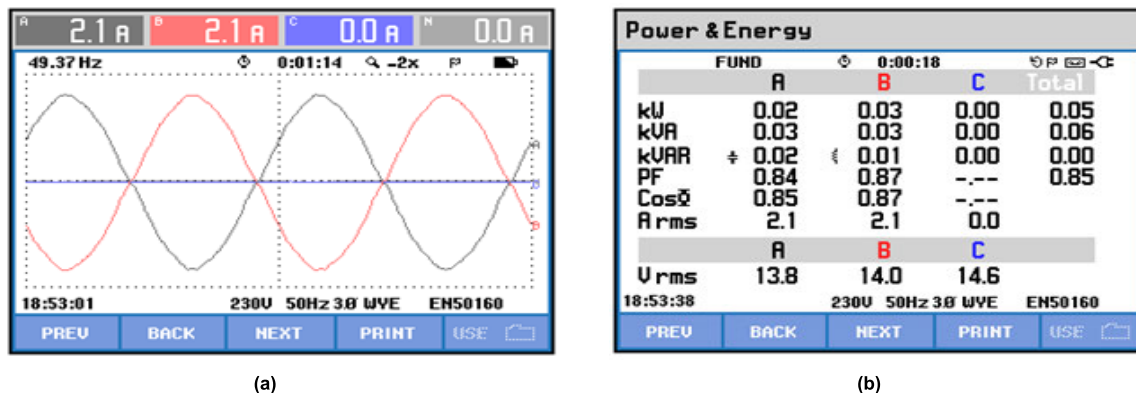


FIGURE 19. (a) Unbalanced load current (b) Performance parameters in completely unbalanced loading condition using the proposed hybrid filter.

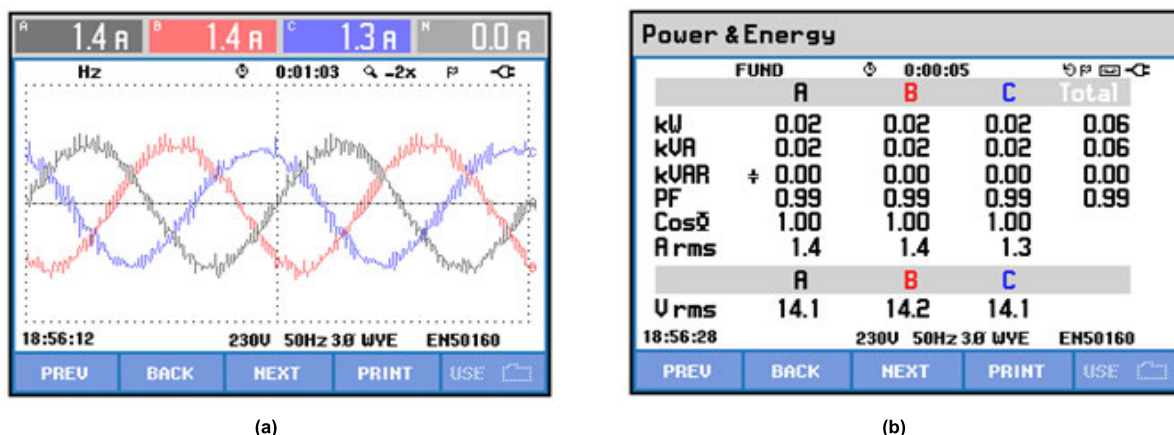


FIGURE 20. (a) Compensated source current (b) Performance parameter after compensation using the proposed hybrid filter.

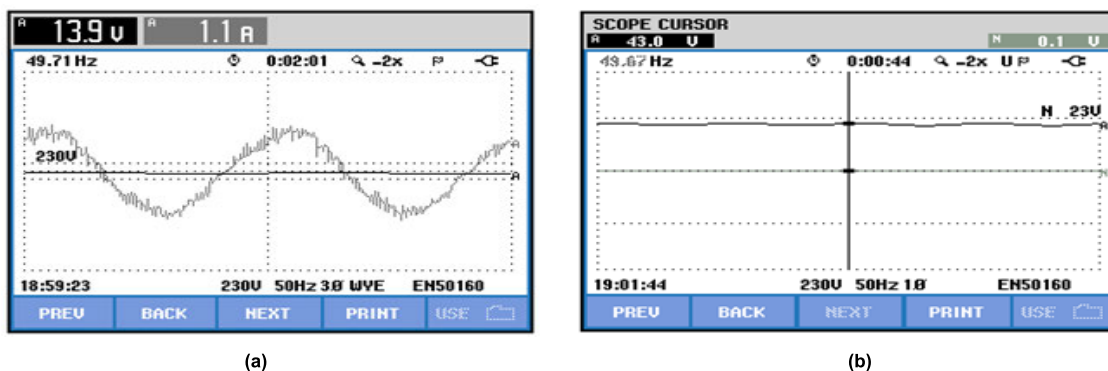


FIGURE 21. (a) Injected filter current (b) Regulated capacitor voltage using the proposed hybrid filter.

The power and power factor before filtering is given in Figure 13 (b). Now, to improve the system performance, PSO-GWO Optimized FOPIDC based HSAPF is connected to the system. Figures 14(a), (b) give the three phase source current of the hybrid filter system and the harmonic spectrum of phase-a current. THD of the source current is reduced from 29.2% to 5.7%. The power and the power factor are given in the Figure 15 (a) which shows that before filtering the power

factor is 0.95 (from Figure 13(b)) and this is improved to 0.99 after the proposed hybrid filter is connected. Injected active filter current is also shown in Figure 15 (b).

A. UNBALANCE LOADING CONDITION

For creating unbalance condition, a single phase lamp load is connected between two lines at the input of the diode bridge rectifier, so that the currents drawn by one phase is

TABLE 3. System parameters for simulation.

PARAMETERS	VALUES
SOURCE VOLTAGE(V _{RMS})	230V
SYSTEM FREQUENCY (F)	50 Hz
SOURCE IMPEDANCES: SOURCE RESISTANCE (R _S) SOURCE INDUCTANCE (L _S)	0.1 OHMS 0.5MH
NON-LINEAR LOAD: DIODE RECTIFIER LOAD RESISTANCE (R _L)	6-DIODE 40 OHMS
UNBALANCED LOAD: LOAD RESISTANCE (R _L)	40 OHMS
SHUNT ACTIVE POWER FILTER: POWER CONVERTER FILTER RESISTANCE (R _C) FILTER INDUCTANCE (L _C) DC-SIDE CAPACITANCE (C _{DC}) REFERENCE VOLTAGE (V _{DC, REF})	6-MOSFETS/6-DIODES 0.4 OHMS 1.35MH 2000 μF 680V
SHUNT PASSIVE POWER FILTER: 5TH HARMONIC FILTER 7TH HARMONIC FILTER 11TH AND 13TH HARMONIC FILTER	kVAR = 1, QUALITY FACTOR Q=50 kVAR = 0.5, QUALITY FACTOR Q=50 kVAR = 0.5, QUALITY FACTOR Q=50

different from that of the other two phases. Before compensation, the currents in three phases are 2.6A, 2.6A and 2.0A respectively and seen to be unbalanced as shown in Figure 16 (a)-(b).

After compensation, the currents are 2.4A, 2.5A and 2.3A which are nearly balanced around 2.4A with THD value as shown in the Figure 17(a), (b). Figure 18 (a) depicts the in phase-c source voltage and current while Figure 18 (b) shows the injected active filter current.

B. COMPLETELY UNBALANCE LOADING CONDITION

One of the phase is opened to investigate the performance of the proposed hybrid filter for completely unbalanced load. Here, phase-c is opened so that the load current in phase-c is zero, the current in remaining two phases are 2.1A. Here, the power factor in one phase is lagging and the other is leading before compensation as shown in the Figure 19(a),(b). After the filtering, the currents are seen to be 1.4A, 1.4A and 1.3A in A, B and C phases respectively, and the power factor is improved to almost unity in all the three phases with help of the hybrid filtering as shown in the Figure 20 (a)-(b). Under unbalance condition, active filter current and the dc capacitor voltage is shown in Figure 21 (a)-(b) respectively. In this case, the capacitor voltage is seen to have more voltage ripples compared to the previous cases as the capacitor needs to compensate not only harmonics but also to provide reactive power.

VI. CONCLUSION

In this research work, the implementation of a hybrid shunt active power filter for three phase three wire system has been carried out. The prototype has been designed and developed to eliminate the load generated harmonics and to improve

TABLE 4. System parameter for experimental set up.

PARAMETERS	VALUES	PARAMETERS	VALUES
V _S	20V(PK)	C _{F5} , L _{F5}	50UF, 8.10MH
F	50HZ	C _{F7} , L _{F7}	20UF, 8.27MH
L _C	3MH	C _{F11} , L _{F11}	40UF, 8.63MH
C _{DC}	2200UF	C _{F13} , L _{F13}	30UF, 8.84MH
V _{DC,REF}	42 V		

the input power factor to unity. The developed system is cost effective, simple and easy for implementation for eliminating the load generated harmonics. The simulation and the hardware case studies able to decrease the harmonics and THD level of the source current. It is observed that the proposed hybrid PSO-GWO optimized FOPIDC based Hybrid Shunt Active Power Filter provides better harmonics compensation as compared to the PSO and GWO optimized FOPIDC/CPIDC based HSAPF under different operating scenarios.

APPENDIX

See tables 3 and 4.

REFERENCES

- [1] T. S. Haugan and E. Tedeschi, "Reactive and harmonic compensation using the conservative power theory," in *Proc. 10th Int. Conf. Ecol. Vehicles Renew. Energies (EVER)*, Mar. 2015, pp. 1–8.
- [2] T. P. and Y. N., "Design of current source hybrid power filter for harmonic current compensation," *Simul. Model. Pract. Theory*, vol. 52, pp. 78–91, Mar. 2015.
- [3] A. K. Mishra, M. K. Pathak, and S. Das, "Isolated converter topologies for power factor correction—A comparison," in *Proc. Int. Conf. Energy, Autom. Signal*, Dec. 2011, pp. 1–6.
- [4] O. P. Mahela and A. G. Shaik, "Topological aspects of power quality improvement techniques: A comprehensive overview," *Renew. Sustain. Energy Rev.*, vol. 58, pp. 1129–1142, May 2016.
- [5] R. Arnold, "Solutions to the power quality problem," *Power Eng. J.*, vol. 15, no. 2, pp. 65–73, Apr. 2001.
- [6] H. Akagi, "Trends in active filters for power quality conditioning," *IEEE Trans. Ind. Appl.*, vol. 32, no. 6, pp. 1312–1322, Nov./Dec. 1996.
- [7] B. Singh, V. Verma, A. Chandra, and K. Al-Haddad, "Hybrid filters for power quality improvement," *IEE Proc. Gener., Transmiss. Distrib.*, vol. 152, no. 3, pp. 365–378, May 2005.
- [8] R. Zahira and A. Peer Fathima, "A technical survey on control strategies of active filter for harmonic suppression," *Procedia Eng.*, vol. 30, pp. 686–693, Jan. 2012.
- [9] A. Bhattacharya, C. Chakraborty, and S. Bhattacharya, "Shunt compensation," *IEEE Ind. Electron. Mag.*, vol. 3, no. 3, pp. 38–49, Sep-2009.
- [10] S. Buso, L. Malesani, and P. Mattavelli, "Comparison of current control techniques for active filter applications," *IEEE Trans. Ind. Electron.*, vol. 45, no. 5, pp. 722–729, Oct. 1998.
- [11] Z. Shuai, A. Luo, C. Tu, and D. Liu, "New control method of injection-type hybrid active power filter," *IET Power Electron.*, vol. 4, no. 9, p. 1051, Nov. 2011.
- [12] M. Kale and E. Özdemir, "Harmonic and reactive power compensation with shunt active power filter under non-ideal mains voltage," *Electr. Power Syst. Res.*, vol. 74, no. 3, pp. 363–370, Jun. 2005.
- [13] M. El-Habrouk, M. K. Darwish, and P. Mehta, "Active power filters: A review," *IEE Proc. Electr. Power Appl.*, vol. 147, no. 5, pp. 13–403, Sep-2000.
- [14] R. El Shatshat, M. Kazerani, and M. M. A. Salama, "Power quality improvement in 3-phase 3-wire distribution systems using modular active power filter," *Electr. Power Syst. Res.*, vol. 61, no. 3, pp. 185–194, Apr. 2002.
- [15] H. Akagi, E. H. Watanabe, and M. Aredes, *Instantaneous Power Theory and Applications to Power Conditioning*. Piscataway, NJ, USA: IEEE Press, 2007.

- [16] H. Akagi, "Active harmonic filters," *Proc. IEEE*, vol. 93, no. 12, pp. 2128–2141, Dec. 2005.
- [17] F. Z. Peng, H. Akagi, and A. Nabae, "A novel harmonic power filter," in *Proc. Rec. 19th Annu. IEEE Power Electron. Spec. Conf. (PESC)*, Apr. 1988, pp. 1151–1158.
- [18] W. M. Grady, M. J. Samotyj, and A. H. Noyola, "Survey of active power line conditioning methodologies," *IEEE Trans. Power Del.*, vol. 5, no. 3, pp. 1536–1542, Jul. 1990.
- [19] M. I. M. Montero, E. R. Cadaval, and F. B. Gonzalez, "Comparison of control strategies for shunt active power filters in three-phase four-wire systems," *IEEE Trans. Power Electron.*, vol. 22, no. 1, pp. 229–236, Jan. 2007.
- [20] R. S. Herrera, P. Salmerón, and H. Kim, "Instantaneous reactive power theory applied to active power filter compensation: Different approaches, assessment, and experimental results," *IEEE Trans. Ind. Electron.*, vol. 55, no. 1, pp. 184–196, Jan. 2008.
- [21] R. A. Hooshmand and M. Torabian Esfahani, "Adaptive filter design based on the LMS algorithm for delay elimination in TCR/FC compensators," *ISA Trans.*, vol. 50, no. 2, pp. 142–149, Apr. 2011.
- [22] L. S. Czarnecki, "Instantaneous reactive power p-q theory and power properties of three-phase systems," *IEEE Trans. Power Del.*, vol. 21, no. 1, pp. 362–367, Jan. 2006.
- [23] S. Kim and P. N. Enjeti, "A new hybrid active power filter (APF) topology," *IEEE Trans. Power Electron.*, vol. 17, no. 1, pp. 48–54, Jan. 2002.
- [24] D. Rivas, L. Moran, J. Dixon, and J. Espinoza, "A simple control scheme for hybrid active power filter," *IEE Proc. Gener., Transmiss. Distrib.*, vol. 149, no. 4, pp. 485–490, Jul. 2002.
- [25] A. Luo, Z. Shuai, W. Zhu, R. Fan, and C. Tu, "Development of hybrid active power filter based on the adaptive fuzzy dividing frequency-control method," *IEEE Trans. Power Del.*, vol. 24, no. 1, pp. 424–432, Jan. 2009.
- [26] V. F. Corasaniti, M. B. Barbieri, P. L. Arnera, and M. I. Valla, "Hybrid power filter to enhance power quality in a medium-voltage distribution network," *IEEE Trans. Ind. Electron.*, vol. 56, no. 8, pp. 2885–2893, Aug. 2009.
- [27] A. Bhattacharya, C. Chakraborty, and S. Bhattacharya, "Parallel-connected shunt hybrid active power filters operating at different switching frequencies for improved performance," *IEEE Trans. Ind. Electron.*, vol. 59, no. 11, pp. 4007–4019, Nov. 2012.
- [28] S. Rahmani, A. Hamadi, and K. Al-Haddad, "A Lyapunov-function-based control for a three-phase shunt hybrid active filter," *IEEE Trans. Ind. Electron.*, vol. 59, no. 3, pp. 1418–1429, Mar. 2012.
- [29] S. Mikkili and A. K. Panda, "PI and fuzzy logic controller based 3-Phase 4-Wire shunt active filters for the mitigation of current harmonics with the i_d - I_q control strategy," *J. Power Electron.*, vol. 11, no. 6, pp. 914–921, Nov. 2011.
- [30] A. Bhattacharya and C. Chakraborty, "A shunt active power filter with enhanced performance using ANN-based predictive and adaptive controllers," *IEEE Trans. Ind. Electron.*, vol. 58, no. 2, pp. 421–428, Feb. 2011.
- [31] S. R. Das, P. K. Ray, A. Mohanty, and T. K. Panigrahi, "Application of artificial intelligence techniques for improvement of power quality using hybrid filters," in *Computational Intelligence in Data Mining*. Singapore: Springer, 2020, pp. 719–729.
- [32] Z. Bingul and O. Karahan, "Comparison of PID and FOPID controllers tuned by PSO and ABC algorithms for unstable and integrating systems with time delay," *Optim. Control Appl. Methods*, vol. 39, no. 4, pp. 1431–1450, Jul. 2018.
- [33] K. J. Åström and T. Hägglund, "The future of PID control," *Control Eng. Pract.*, vol. 9, no. 11, pp. 1163–1175, Nov. 2001.
- [34] K. N. A. Rani, M. F. Abdulmalek, and S. Neoh, "Nature-inspired cuckoo search algorithm for side lobe suppression in a symmetric linear antenna array," *Radio Eng. J.*, vol. 21, no. 3, pp. 865–874, Sep. 2012.
- [35] K. J. Astrom and T. Haggglund, *PID Controllers: Theory, Design and Tuning*, 2nd ed. Research Triangle Park, NC, USA: Instrument Society of America, 1995.
- [36] Z. Wang, Q. Su, and X. Luo, "A novel HTD-CS based PID controller tuning method for time delay continuous systems with multi-objective and multi-constraint optimization," *Chem. Eng. Res. Des.*, vol. 115, pp. 98–106, Nov. 2016.
- [37] A. Herreros, E. Baeyens, and J. R. Perán, "Design of PID-type controllers using multiobjective genetic algorithms," *ISA Trans.*, vol. 41, no. 4, pp. 457–472, Oct. 2002.
- [38] L. Chaib, A. Choucha, and S. Arif, "Optimal design and tuning of novel fractional order PID power system stabilizer using a new Metaheuristic bat algorithm," *Ain Shams Eng. J.*, vol. 8, no. 2, pp. 113–125, Jun. 2017.
- [39] D. Valério and J. S. da Costa, "Tuning of fractional PID controllers with Ziegler–Nichols-type rules," *Signal Process.*, vol. 86, no. 10, pp. 2771–2784, Oct. 2006.
- [40] J. Kennedy and R. Eberhart, "Particle swarm optimization," in *Proc. IEEE Int. Conf. Neural Netw.*, vol. 4, Nov. 1995, pp. 1942–1948.
- [41] S. S. Patnaik and A. K. Panda, "Particle swarm optimization and bacterial foraging optimization techniques for optimal current harmonic mitigation by employing active power filter," *Appl. Comput. Intell. Soft Comput.*, vol. 2012, pp. 1–10, Jan. 2012.
- [42] S. Mirjalili, S. M. Mirjalili, and A. Lewis, "Wolf optimizer," *Adv. Eng. Softw.*, vol. 69, pp. 46–61, 2014.
- [43] R. K. Mallick and N. Nahak, "Grey wolves-based optimization technique for tuning damping controller parameters of unified power flow controller," in *Proc. Int. Conf. Electr., Electron., Optim. Techn. (ICEEOT)*, Mar. 2016, pp. 1458–1463.
- [44] N. Nahak and R. K. Mallick, "Enhancement of small signal stability of power system using UPFC based damping controller with novel optimized fuzzy PID controller," *J. Intell. Fuzzy Syst.*, vol. 35, no. 1, pp. 501–512, Jul. 2018.
- [45] A. Nabae, S. Ogasawara, and H. Akagi, "A novel control scheme for current-controlled PWM inverters," *IEEE Trans. Ind. Appl.*, vol. IA-22, no. 4, pp. 697–701, Jul. 1986.
- [46] D. M. Brod and D. W. Novotny, "Current control of VSI-PWM inverters," *IEEE Trans. Ind. Appl.*, vol. IA-21, no. 3, pp. 562–570, May 1985.
- [47] J. Zeng, C. Yu, Q. Qi, Z. Yan, Y. Ni, B. L. Zhang, S. Chen, and F. F. Wu, "A novel hysteresis current control for active power filter with constant frequency," *Electr. power Syst. research.*, vol. 68, no. 1, pp. 75–82, Jan. 2004.



ALOK KUMAR MISHRA received the M.Tech. degree from IIT Roorkee, India, in 2011. He is currently pursuing the Ph.D. degree with SOA University, Bhubaneswar, Odisha, India. He is currently working as an Assistant Professor with the Department of EEE, Institute of Technical Education and Research (ITER), SOA Deemed to be University. His main research interests include power electronics, drives and control, robust control, power electronics converters, facts devices, power quality, and biomedical engineering.



SOUMYA RANJAN DAS (Graduate Student Member) is currently pursuing the Ph.D. degree with the Electrical Engineering Department, International Institute of Information Technology (IIIT), Bhubaneswar. He has authored several research articles in international journals and conferences, and one textbook with Wiley publication. His research interests include distributed generation and custom power device-based power quality analysis and design of interfacing converters for renewable energy resources.



PRAKASH K. RAY (Senior Member, IEEE) received the Ph.D. degree from MNNIT, Allahabad, India, in 2012. He completed the Post-doctoral Fellowship from Nanyang Technological University (NTU), Singapore, in 2018. He is currently working as an Associate Professor with the Department of Electrical Engineering, CET, Bhubaneswar, India. He has published more than 100 technical articles in international conferences and refereed journals. His research interests include distributed generations, digital signal processing, and soft computing applications in power systems and power quality. He is a Life Member of the Indian Society for Technical Education (LMISTE).



RANJAN KUMAR MALLICK was born in India, in 1972. He received the bachelor's degree in electrical engineering from the Institution of Engineers, India, in 1996, the M.E. degree in power system engineering from VSSUT, Burla, Odisha, in 2001, and the Ph.D. degree from BPUT, Odisha, in 2013. He is currently working as a Professor with the Department of Electrical and Electronics Engineering, ITER, SOA University, Odisha, India. He is having 17 years of experience in teaching and research. His research interests include the application of power electronics, optimization techniques in power systems, economic load dispatch, and the design and control of HVDC converters.



ASIT MOHANTY (Member, IEEE) was graduated from NIT Durgapur. He is currently with the Electrical Engineering Department, CET, Bhubaneswar. He has four long years of research experience from MNNIT Allahabad. He has more than 15 years of experiences in teaching and research. His research interests include modeling and control of distributed energy sources, power system stability and control, power quality, and soft computing applications in power systems.

He is a Life Member of the Indian Society for Technical Education (LMISTE).



DILLIP K. MISHRA (Graduate Student Member) received the M.Tech. (Hons.) degree from the College of Engineering and Technology (CET), Bhubaneswar, India.

He has been working in academia as well as industry for more than six years in India. He is currently with the University of Technology Sydney, Sydney, Australia. He has authored around 30 research articles in international journals and conferences, and one textbook with Wiley publication.

His areas of research interests include automatic generation control, renewable energy system integration, microgrid, solid-state transformer, and power system reliability/resiliency.

...